

Sorting out quenched jets

Jasmine Brewer,^{1,*} José Guilherme Milhano,^{2,3,†} and Jesse Thaler^{1,4,‡}

¹*Center for Theoretical Physics, Massachusetts Institute of Technology, Cambridge, MA 02139, USA*

²*LIP, Av. Prof. Gama Pinto, 2, P-1649-003 Lisboa, Portugal*

³*Instituto Superior Técnico (IST), Universidade de Lisboa, Av. Rovisco Pais 1, 1049-001, Lisbon, Portugal*

⁴*Department of Physics, Harvard University, 17 Oxford Street, Cambridge, MA 02138, USA*

We introduce a new “quantile” analysis strategy to study the modification of jets as they traverse through a droplet of quark-gluon plasma. To date, most jet modification studies have been based on comparing the jet properties measured in heavy-ion collisions to a proton-proton baseline at the same reconstructed jet transverse momentum (p_T). It is well known, however, that the quenching of jets from their interaction with the medium leads to a migration of jets from higher to lower p_T , making it challenging to directly infer the degree and mechanism of jet energy loss. Our proposed quantile matching procedure is inspired by (but not reliant on) the approximate monotonicity of energy loss in the jet p_T . In this strategy, jets in heavy-ion collisions ordered by p_T are viewed as modified versions of the same number of highest-energy jets in proton-proton collisions, and the fractional energy loss as a function of jet p_T is a natural observable (Q_{AA}). Furthermore, despite non-monotonic fluctuations in the energy loss, we use an event generator to validate the strong correlation between the p_T of the parton that initiates a heavy-ion jet and the p_T of the vacuum jet which corresponds to it via the quantile procedure (p_T^{quant}). We demonstrate that this strategy both provides a complementary way to study jet modification and mitigates the effect of p_T migration in heavy-ion collisions.

The deconfined phase of QCD matter, the quark-gluon plasma, was first discovered in collisions of heavy nuclei at the Relativistic Heavy Ion Collider [1–5] and confirmed at the Large Hadron Collider [6–8]. As in high-energy proton-proton collisions, heavy-ion collisions produce collimated sprays of particles, called jets, from highly energetic scatterings of quarks and gluons. The observation of “jet quenching”—a strong suppression and modification of jets in heavy-ion collisions [7–9]—ushered in a new era of studying the properties of the quark-gluon plasma by measuring its effect on jets [10–23].

A central issue in interpreting jet quenching measurements is that medium-induced modifications necessarily affect how jets are identified experimentally. Current methods compare proton-proton and heavy-ion jets of the same final (reconstructed) transverse momentum p_T and, as such, inevitably suffer from significant biases from the migration of jets from higher to lower p_T due to medium-induced energy loss (see [24, 25]). While these methods have been very successful in qualitatively demonstrating the phenomena of jet quenching, quantitative studies often necessitate interpreting the data through theoretical models which include migration effects. Ideally, one would like to isolate samples of jets in proton-proton and heavy-ion collisions which were statistically equivalent when they were produced, differing only by the effects of the plasma.

In this Letter, we propose a novel data-driven strategy for comparing heavy-ion (AA) jet measurements to proton-proton (pp) baselines which mitigates, to a large extent, the effect of p_T migration. The famous jet ratio R_{AA} compares the effective cross-section for jets in proton-proton and heavy-ion collisions with the same re-

constructed p_T :

$$R_{AA} = \left. \frac{\sigma_{AA}^{\text{eff}}}{\sigma_{PP}^{\text{eff}}} \right|_{p_T}, \quad (1)$$

as illustrated in blue in Fig. 1a. Here, we introduce a “quantile” procedure, which divides jet samples sorted by p_T into quantiles of equal probability. Our new proposed observable for heavy-ion collisions is the p_T ratio between heavy-ion and proton-proton jets in the same quantile:

$$Q_{AA} = \left. \frac{p_T^{AA}}{p_T^{PP}} \right|_{\Sigma^{\text{eff}}}, \quad (2)$$

as illustrated in red in Fig. 1b, where $1 - Q_{AA}$ is a proxy for the average fractional jet energy loss. (Q_{AA} is not related to Q_{pA} used by ALICE [29]). Although R_{AA} can be obtained from Q_{AA} if the proton-proton jet spectrum is known, we will see that the physics interpretation of R_{AA} and Q_{AA} can be quite different. Fig. 1a additionally shows the pseudo-quantile \tilde{Q}_{AA} , which is related to the observable S_{loss} introduced by PHENIX for single hadrons [30–32].

To give an intuitive understanding of Eq. (2), consider a simplified scenario where medium-induced energy loss is monotonic in the p_T of the initial unquenched jet. In that case, the n^{th} highest energy jet in a heavy-ion sample is a modified version of the n^{th} highest energy jet in the corresponding proton-proton sample. Thus, in this simplified picture of energy loss, we can obtain a sample of heavy-ion jets that is statistically equivalent to its proton-proton counterpart by selecting jets with the same (upper) cumulative effective cross-section:

$$\Sigma^{\text{eff}}(p_T^{\text{min}}) = \int_{p_T^{\text{min}}}^{\infty} dp_T \frac{d\sigma^{\text{eff}}}{dp_T}. \quad (3)$$

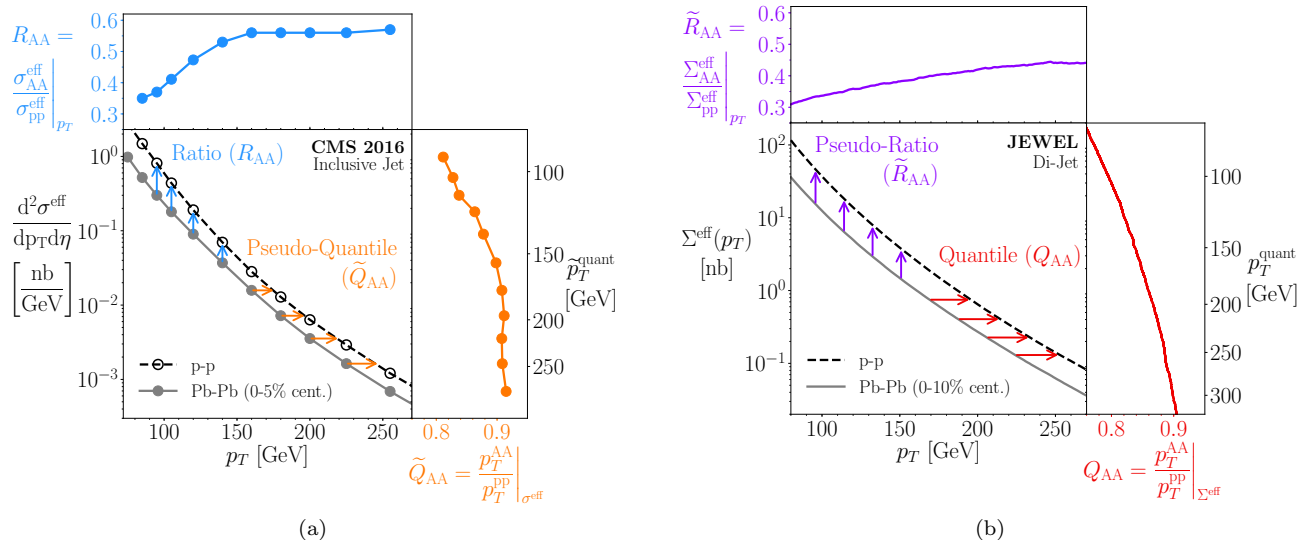


FIG. 1. Illustration comparing the ratio and quantile procedures. (a) The inclusive jet p_T spectra measured by CMS [26], for a jet radius of $R = 0.4$. The standard jet ratio R_{AA} (blue) compares heavy-ion and proton-proton jet cross-sections vertically at the same reconstructed jet p_T . (b) The jet p_T cumulative cross-sections extracted from JEWEL [27, 28]. The quantile procedure Q_{AA} (red) compares heavy-ion and proton-proton jet p_T thresholds horizontally at the same cumulative cross-section. From this, one can map each p_T^{AA} (base of red arrows) into the p_T of proton-proton jets in the same quantile, p_T^{quant} (tip of red arrows). For completeness, we also show the pseudo-quantile \tilde{Q}_{AA} (orange, with corresponding $\tilde{p}_T^{\text{quant}}$) defined on the cross-section and pseudo-ratio \tilde{R}_{AA} (purple) defined on the cumulative cross-section. Though we will not explore the use of \tilde{Q}_{AA} or \tilde{R}_{AA} in the present study, we note that in JEWEL, the values of p_T^{quant} and $\tilde{p}_T^{\text{quant}}$ differ by only a few percent.

Note that for comparison to proton-proton cross-sections, heavy-ion cross-sections must be rescaled by the average number of nucleon-nucleon collisions $\langle N_{\text{coll}} \rangle$: $\sigma_{\text{pp}}^{\text{eff}} = \sigma_{\text{pp}}$, $\sigma_{\text{AA}}^{\text{eff}} = \sigma_{\text{AA}} / \langle N_{\text{coll}} \rangle$. Of course, energy loss is not strictly monotonic in p_T , since other properties of a jet and of the jet-medium interaction influence its energy loss and cause jets with the same initial p_T to lose different fractions of their energy. Below, we will quantify the usefulness of this quantile picture in the context of a realistic event generator where significant non-monotonicities are indeed present.

Due to the steeply-falling jet production spectrum ($\sigma \sim p_T^{-6}$), jets within a given range in reconstructed heavy-ion p_T are dominated by those which were least modified (see e.g. [33]). Addressing this issue requires comparing jets that had the same p_T when they were initially produced. In rarer events where an energetic γ or Z boson is produced back-to-back with a jet, the unmodified boson energy approximates the initial energy of the recoiling jet [15, 34]. In general jet events, however, the jet energy before medium effects cannot be measured.

A key result of this work is that the quantile picture also provides a natural proxy for the unmodified jet p_T that is observable in general jet events. Given a heavy-ion jet with reconstructed momentum p_T^{AA} , we can define p_T^{quant} implicitly as the momentum of a proton-proton jet

with the same (upper) cumulative cross-section:

$$\Sigma_{\text{pp}}^{\text{eff}}(p_T^{\text{quant}}) \equiv \Sigma_{\text{AA}}^{\text{eff}}(p_T^{AA}). \quad (4)$$

In this quantile picture, p_T^{quant} is viewed as the initial jet p_T prior to medium effects. The mapping from p_T^{AA} to p_T^{quant} is illustrated by the red arrows in Fig. 1b, with $p_T^{AA} = p_T^{\text{quant}} Q_{AA}(p_T^{\text{quant}})$. Intriguingly, we will show that p_T^{quant} approximates the p_T of a heavy-ion jet before quenching with comparable fidelity to the unmodified boson energy p_T^Z available only in rarer Z +jet events. In particular, comparing properties of proton-proton and heavy-ion jet samples with the same p_T^{quant} may substantially enhance the sensitivity of modification observables by targeting jets that were more strongly modified.

For the remainder of this work, we consider samples of Z +jet and di-jet events in the heavy-ion Monte Carlo event generator JEWEL 2.1.0 [27, 28], based on vacuum jet production in PYTHIA 6 [35]. For each process, we generate 2 million each of proton-proton and head-on (0–10% centrality) heavy-ion events at 2.76 TeV and reconstruct anti- k_t jets using FASTJET 3.3.0 [36, 37] with radius parameter $R = 0.4$ and pseudorapidity $|\eta| < 2$. We include initial state radiation but do not include medium recoils, since medium response is not expected to have a significant effect on Eq. (3) at the values of p_T^{min} considered here. For Z +jet events we identify the Z from its decay to muons and consider the leading recoiling jet,

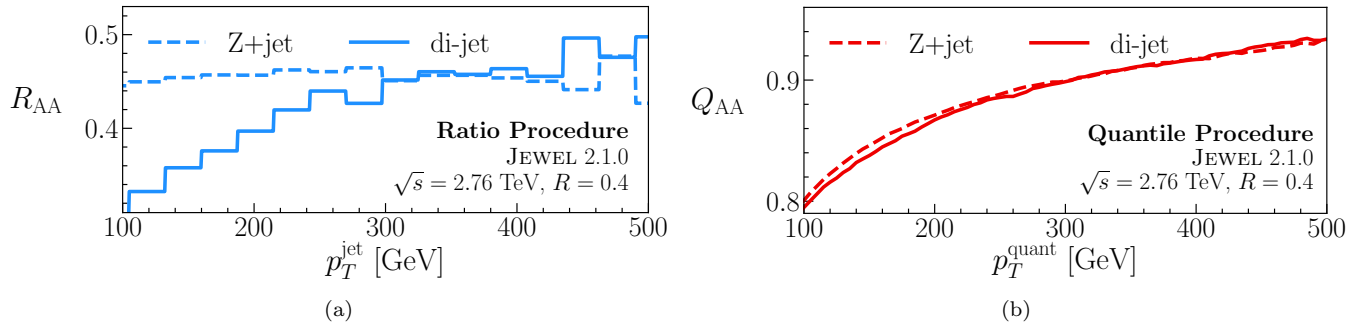


FIG. 2. Distributions of (a) R_{AA} as a function of p_T^{jet} and (b) Q_{AA} as a function of p_T^{quant} , for the Z+jet (dashed) and di-jet (solid) samples in JEWEL. Although R_{AA} and Q_{AA} are derived from the same underlying jet p_T spectra, they provide different and complementary information. For example, the p_T dependence of R_{AA} is very different for Z+jet and di-jet events in JEWEL, while the average fractional p_T loss $1 - Q_{AA}$ is similar. Note that R_{AA} requires binning of the data, while Q_{AA} , which is based on the cumulative cross-section, can be plotted unbinned.

and for di-jet events we consider the two highest- p_T jets. We consider Z+jet instead of γ +jet events to avoid introducing additional cuts to isolate prompt photons which could bias the validation. The default heavy-ion background in JEWEL is a Bjorken expanding medium with initial peak temperature $T_i = 485$ MeV and formation time $\tau_i = 0.6$ fm, consistent with the parameters used to fit data at 2.76 TeV in more realistic hydrodynamic simulations [28, 38].

Using these Z+jet and di-jet samples from JEWEL, Fig. 2a shows the standard R_{AA} (also called I_{AA} for Z+jet) and Fig. 2b shows the p_T ratio Q_{AA} . Although the R_{AA} for Z+jet and di-jet events have significantly different p_T -dependence, it is interesting that the average fractional energy loss of jets is very similar, as quantified by $1 - Q_{AA}$. This might be surprising since Z+jet and di-jet events have different fractions of quark and gluon jets, though Ref. [39] suggests that quark and gluon jets may experience similar energy loss in JEWEL; whether this is borne out in data is an open question. Regardless, it is clear that R_{AA} and Q_{AA} offer complementary probes of the jet quenching phenomenon and are therefore both interesting observables in their own right. The quantile procedure also shows that the highest- p_T jets lose a small fraction of their energy on average ($(1 - Q_{AA}) \sim 5\%$), even though R_{AA} is far below one. This result can be compared to other methods for extracting the average energy loss from data, for example Ref. [40].

We now turn to validating the interpretation of p_T^{quant} as a proxy for the initial p_T of a heavy-ion jet before quenching by the medium. In Z+jet events, p_T^Z can be used as a baseline for the (approximate) initial p_T of the leading recoiling jet, since the Z boson does not interact with the quark-gluon plasma. For a given value of p_T^Z , there is a distribution of recoil jet momenta whose mean is shown in the upper panel of Fig. 3a. Even in proton-proton collisions, the recoiling jet p_T is systematically lower on average than p_T^Z due to out-of-cone radiation

and events with multiple jets. In heavy-ion collisions, it is even lower due to energy loss. Intriguingly, the mean value of p_T^{quant} (red) is much more comparable to that of p_T^{PP} (dashed black) than p_T^{AA} (blue) is, indicating that p_T^{quant} is a good proxy for the initial jet p_T . On the other hand, the standard deviation of p_T^{quant} , shown in the lower panel of Fig. 3a, is higher than that of p_T^{PP} due to energy loss fluctuations. These cannot be undone by the quantile procedure, which can only give a perfect reconstruction of the distribution of p_T^{PP} in the case of strictly monotonic energy loss.

We emphasize that the distribution in Fig. 3a is physically observable and could be used to validate the quantile procedure in experimental data. Crucially, quantile matching can also provide a baseline for the initial jet p_T in general jet events. To validate this in di-jet events at the generator level, we use the p_T of the partons from the initial hard matrix element in JEWEL, p_T^{MC} , as an (unphysical and unobservable) baseline for the initial jet p_T (see [41]). We consider the two highest- p_T jets and match each jet with the p_T^{MC} that minimizes $\Delta R = \sqrt{\Delta\eta^2 + \Delta\phi^2}$ between the jet and the parton. Each of the two jets then enters independently in Fig. 3b, which demonstrates the correlation of the jet p_T to p_T^{MC} for proton-proton and heavy-ion jets, with the results of the quantile procedure in red. Fig. 3b is the only figure in this work that involves an unobservable quantity, and it shows remarkably similar features to Fig. 3a which can be measured experimentally.

It might be surprising that the curves in Fig. 3 are fairly flat as a function of the baseline initial p_T . This can be understood, however, from a minimal model in which the final energy of a jet is obtained from its initial energy via gaussian smearing. Consider the probability

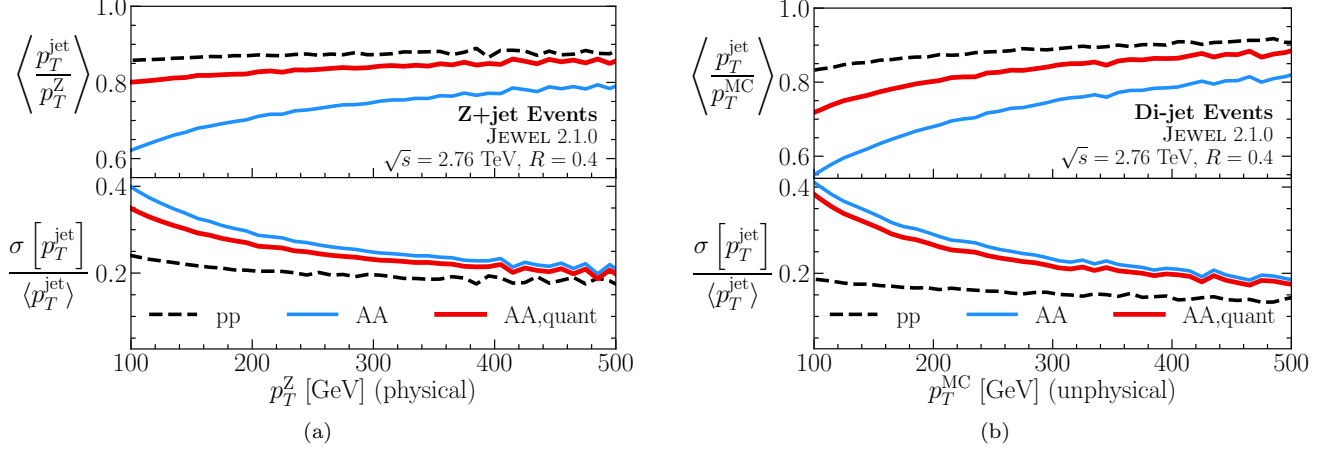


FIG. 3. Mean of the jet p_T distribution compared to a baseline initial p_T (top), along with the corresponding standard deviation (bottom). Shown are (a) Z+jet events where the baseline is the physically observable p_T of the recoiling Z boson and (b) di-jet events where the baseline is the unphysical and unobservable p_T^{MC} of the initial hard scattering obtained from JEWEL. The reconstructed jet p_T for proton-proton and heavy-ion jets are shown in dashed black and blue, respectively. The p_T^{quant} of the heavy-ion sample, shown in red, more closely matches the initial jet p_T than the reconstructed heavy-ion p_T does.

distribution

$$p(p_T^{\text{AA}}|p_T^{\text{in}}) = \int dp_T^{\text{PP}} \mathcal{N}(p_T^{\text{AA}}|\tilde{\mu}_2 p_T^{\text{PP}}, \tilde{\sigma}_2 p_T^{\text{PP}}) \times \mathcal{N}(p_T^{\text{PP}}|\tilde{\mu}_1 p_T^{\text{in}}, \tilde{\sigma}_1 p_T^{\text{in}}). \quad (5)$$

Here, $\mathcal{N}(x|\mu, \sigma)$ is a normal distribution in the variable x with mean μ and standard deviation σ , and $\tilde{\mu}_{1,2}$ and $\tilde{\sigma}_{1,2}$ are dimensionless constants. Eq. (5) describes the probabilistic relation between the seed-parton momentum p_T^{in} (interpreted as p_T^Z or p_T^{MC}) and the quenched momentum p_T^{AA} via two stages of gaussian smearing: first from p_T^{in} to the unquenched jet momentum p_T^{PP} , and then from p_T^{PP} to the quenched momentum p_T^{AA} . Integrating over intermediate values of p_T^{PP} gives $p(p_T^{\text{AA}}|p_T^{\text{in}})$, the probability of p_T^{AA} for fixed p_T^{in} . This is an example of a model in which the average energy loss is monotonic in p_T , since $\mu_2 = \tilde{\mu}_2 p_T^{\text{PP}}$ is a monotonic function of p_T^{PP} , but energy loss is not monotonic in p_T jet-by-jet since $\tilde{\sigma}_2 \neq 0$.

The mean and standard deviation of the distribution in Eq. (5) can be calculated analytically (see [42]):

$$\begin{aligned} \langle p_T^{\text{AA}}/p_T^{\text{in}} \rangle &= \tilde{\mu}_1 \tilde{\mu}_2, \\ \sigma(p_T^{\text{AA}}/p_T^{\text{in}}) &= \sqrt{\tilde{\mu}_1^2 \tilde{\sigma}_2^2 + \tilde{\mu}_2^2 \tilde{\sigma}_1^2 + \tilde{\sigma}_1^2 \tilde{\sigma}_2^2}, \end{aligned} \quad (6)$$

though the resulting distribution is not generally gaussian. These can be compared to the upper and lower panels, respectively, of Fig. 3. The fact that Eq. (6) has no p_T^{in} -dependence is consistent with the fact that the curves in Fig. 3 are approximately flat. To the extent that this model is semi-realistic, Eq. (6) and a measurement of Fig. 3a would provide an estimate of the average energy loss and the size of energy loss fluctuations. Taking approximate values from Fig. 3a at $p_T^Z = 300$ GeV of

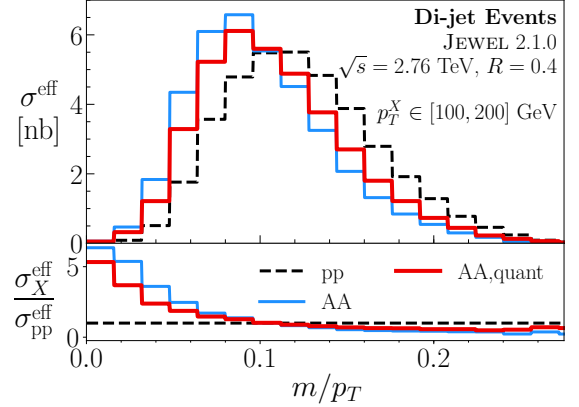


FIG. 4. Distribution of m/p_T for proton-proton (dashed black) and heavy-ion (blue) jets in di-jet events with reconstructed $p_T \in [100, 200]$ GeV. Heavy-ion jets with $p_T^{\text{quant}} \in [100, 200]$ GeV, corresponding to $p_T^{\text{AA}} \in [80, 173]$ GeV, are in red. The heavy-ion result is normalized to match the proton-proton baseline but the quantile result has the correct normalization by construction. Partially compensating for p_T migration via the quantile procedure shifts m/p_T towards being less modified.

$\langle p_T^{\text{PP}}/p_T^Z \rangle \equiv \tilde{\mu}_1 \approx 0.87$, $\sigma(p_T^{\text{PP}}/p_T^{\text{in}}) \equiv \tilde{\sigma}_1 \approx 0.2 \tilde{\mu}_1 = 0.17$, $\langle p_T^{\text{AA}}/p_T^Z \rangle \approx 0.74$, and $\sigma(p_T^{\text{AA}}/p_T^Z) \approx 0.24 \langle p_T^{\text{AA}}/p_T^Z \rangle = 0.18$, Eq. (6) yields $\tilde{\mu}_2 \approx 0.85$ and $\tilde{\sigma}_2 \approx 0.12$. It is satisfying that this extracted $\tilde{\mu}_2$ value is comparable to Q_{AA} in Fig. 2b, which is a more direct proxy for fractional energy loss.

As a final application in this Letter, we demonstrate how the quantile procedure can be used to characterize the effects of p_T migration via an example jet substructure observable, the dimensionless ratio of the jet mass

to its reconstructed p_T , m/p_T . Fig. 4 shows distributions of m/p_T for proton-proton and heavy-ion jets in a range of reconstructed p_T in dashed black and blue, respectively. Heavy-ion jets with that range of p_T^{quant} are those in the same quantile as the proton-proton baseline, and m/p_T for that sample is shown in red. For the purpose of this example, we define m/p_T from the reconstructed jet mass and p_T , such that the effect of the quantile procedure is only to change the p_T range of jets in the selection. Using the quantile procedure to (partially) account for the migration of jets to lower p_T , the red distribution shifts toward m/p_T being less modified. We note that the jet mass is known to have significant corrections from medium response [43, 44] so this should be taken only as an illustrative example.

In conclusion, we introduced a new strategy for comparing heavy-ion jets to a baseline of proton-proton jets in the same quantile when sorted by p_T . As shown in Fig. 2, our new Q_{AA} observable is based on the same jet p_T spectra as R_{AA} but exposes different and complementary information. As shown in Fig. 3, our new p_T^{quant} observable is closely correlated with the initial p_T a heavy-ion jet had before energy loss to the plasma. Thus, the quantile procedure provides a data-driven way to study the modification of quenched jets and minimize the effects of sample migration. Experimental tests in Z+jet or γ +jet can validate the effectiveness of p_T^{quant} as a proxy for the initial p_T of a heavy-ion jet. If these tests are successful, the quantile procedure can then be used to re-analyze measurements of jet modification observables in general jet events with an aim toward characterizing and minimizing p_T migration effects and thus compare jet samples that were born alike. The measurement of Q_{AA} will provide information on the functional form of the average energy loss which would further constrain theoretical models. It can also be used to measure differences in average energy loss between quark- and gluon-dominated jet samples. Measurements of Q_{AA} with jet grooming [45–49] may also elucidate, for example, how energy is lost by the hard core of a jet compared to the diffuse periphery. It would also be interesting to study the application of this procedure to understanding energy loss fluctuations. Finally, Fig. 1 shows two additional observables—the pseudo-ratio \tilde{R}_{AA} and pseudo-quantile \tilde{Q}_{AA} —which may be relevant for experimental applications.

We thank Liliana Apolinário, Yang-Ting Chien, Yen-Jie Lee, William Lewis, James Mulligan, Aditya Parikh, Krishna Rajagopal, Gavin Salam, Andrew Turner, and Korinna Zapp for helpful discussions. JB and JT are supported by the U.S. Department of Energy, Office of Science, Office of Nuclear Physics under grant Contract Number de-sc0011090 and the Office of High Energy Physics under grant Contract Number de-sc0012567. JT is also supported by the Simons Foundation through a Simons Fellowship in Theoretical Physics, and he thanks

the Harvard Center for the Fundamental Laws of Nature for hospitality while this work was completed. GM is supported by Fundação para a Ciência e a Tecnologia (Portugal) under project CERN/FIS-PAR/0022/2017, and he gratefully acknowledges the hospitality of the CERN theory group.

* jtbrewer@mit.edu

† guilherme.milhano@tecnico.ulisboa.pt

‡ jthaler@mit.edu

- [1] C. Adler et al. (STAR), Phys. Rev. Lett. **87**, 182301 (2001), nucl-ex/0107003.
- [2] I. Arsene et al. (BRAHMS), Nucl. Phys. **A757**, 1 (2005), nucl-ex/0410020.
- [3] B. B. Back et al., Nucl. Phys. **A757**, 28 (2005), nucl-ex/0410022.
- [4] K. Adcox et al. (PHENIX), Nucl. Phys. **A757**, 184 (2005), nucl-ex/0410003.
- [5] J. Adams et al. (STAR), Nucl. Phys. **A757**, 102 (2005), nucl-ex/0501009.
- [6] K. Aamodt et al. (ALICE), Phys. Rev. Lett. **105**, 252302 (2010), 1011.3914.
- [7] G. Aad et al. (ATLAS), Phys. Rev. Lett. **105**, 252303 (2010), 1011.6182.
- [8] S. Chatrchyan et al. (CMS), Phys. Rev. **C84**, 024906 (2011), 1102.1957.
- [9] J. Adam et al. (ALICE), Phys. Lett. **B746**, 1 (2015), 1502.01689.
- [10] D. A. Appel, Phys. Rev. **D33**, 717 (1986).
- [11] J. P. Blaizot and L. D. McLerran, Phys. Rev. **D34**, 2739 (1986).
- [12] M. Gyulassy and M. Plumer, Phys. Lett. **B243**, 432 (1990).
- [13] X.-N. Wang and M. Gyulassy, Phys. Rev. Lett. **68**, 1480 (1992).
- [14] S. Chatrchyan et al. (CMS), Phys. Lett. **B712**, 176 (2012), 1202.5022.
- [15] S. Chatrchyan et al. (CMS), Phys. Lett. **B718**, 773 (2013), 1205.0206.
- [16] S. Chatrchyan et al. (CMS), Phys. Rev. Lett. **113**, 132301 (2014), [Erratum: Phys. Rev. Lett.115,no.2,029903(2015)], 1312.4198.
- [17] S. Chatrchyan et al. (CMS), Phys. Rev. **C90**, 024908 (2014), 1406.0932.
- [18] V. Khachatryan et al. (CMS), JHEP **01**, 006 (2016), 1509.09029.
- [19] M. Aaboud et al. (ATLAS), Phys. Lett. **B774**, 379 (2017), 1706.09363.
- [20] S. Acharya et al. (ALICE), Phys. Lett. **B776**, 249 (2018), 1702.00804.
- [21] M. Aaboud et al. (ATLAS) (2018), 1805.05635.
- [22] M. Aaboud et al. (ATLAS), Phys. Rev. **C98**, 024908 (2018), 1805.05424.
- [23] S. Acharya et al. (ALICE), Submitted to: JHEP (2018), 1807.06854.
- [24] J. Casalderrey-Solana and C. A. Salgado, Acta Phys. Polon. **B38**, 3731 (2007), 0712.3443.
- [25] D. d’Enterria, Landolt-Bornstein **23**, 471 (2010), 0902.2011.
- [26] V. Khachatryan et al. (CMS), Phys. Rev. **C96**, 015202

- (2017), 1609.05383.
- [27] K. C. Zapp, Eur. Phys. J. **C74**, 2762 (2014), 1311.0048.
- [28] R. Kunnawalkam Elayavalli and K. C. Zapp, Eur. Phys. J. **C76**, 695 (2016), 1608.03099.
- [29] A. Toia (ALICE), Nucl. Phys. **A926**, 78 (2014), 1403.5143.
- [30] S. S. Adler et al. (PHENIX), Phys. Rev. **C76**, 034904 (2007), nucl-ex/0611007.
- [31] A. Adare et al. (PHENIX), Phys. Rev. **C87**, 034911 (2013), 1208.2254.
- [32] A. Adare et al. (PHENIX), Phys. Rev. **C93**, 024911 (2016), 1509.06735.
- [33] H. A. Andrews et al. (2018), 1808.03689.
- [34] A. M. Sirunyan et al. (CMS), Phys. Rev. Lett. **119**, 082301 (2017), 1702.01060.
- [35] T. Sjostrand, S. Mrenna, and P. Z. Skands, JHEP **05**, 026 (2006), hep-ph/0603175.
- [36] M. Cacciari, G. P. Salam, and G. Soyez, JHEP **04**, 063 (2008), 0802.1189.
- [37] M. Cacciari, G. P. Salam, and G. Soyez, Eur. Phys. J. **C72**, 1896 (2012), 1111.6097.
- [38] C. Shen and U. Heinz, Phys. Rev. **C85**, 054902 (2012), [Erratum: Phys. Rev. **C86**, 049903(2012)], 1202.6620.
- [39] L. Apolinário, J. Barata, and G. Milhano, in *9th International Conference on Hard and Electromagnetic Probes of High-Energy Nuclear Collisions: Hard Probes 2018 (HP2018) Aix-Les-Bains, Savoie, France, October 1-5, 2018* (2018), 1812.06019.
- [40] Y. He, L.-G. Pang, and X.-N. Wang (2018), 1808.05310.
- [41] J. G. Milhano and K. C. Zapp, Eur. Phys. J. **C76**, 288 (2016), 1512.08107.
- [42] C. M. Bishop, *Pattern Recognition and Machine Learning (Information Science and Statistics)* (Springer-Verlag, Berlin, Heidelberg, 2006), ISBN 0387310738.
- [43] R. Kunnawalkam Elayavalli and K. C. Zapp, JHEP **07**, 141 (2017), 1707.01539.
- [44] C. Park, S. Jeon, and C. Gale (2018), 1807.06550.
- [45] J. M. Butterworth, A. R. Davison, M. Rubin, and G. P. Salam, Phys. Rev. Lett. **100**, 242001 (2008), 0802.2470.
- [46] S. D. Ellis, C. K. Vermilion, and J. R. Walsh, Phys. Rev. **D81**, 094023 (2010), 0912.0033.
- [47] D. Krohn, J. Thaler, and L.-T. Wang, JHEP **02**, 084 (2010), 0912.1342.
- [48] M. Dasgupta, A. Fregoso, S. Marzani, and G. P. Salam, JHEP **09**, 029 (2013), 1307.0007.
- [49] A. J. Larkoski, S. Marzani, G. Soyez, and J. Thaler, JHEP **05**, 146 (2014), 1402.2657.